Comparative Study of Chemical, Mechanical, Thermal, and Barrier Properties of Poly(Lactic Acid) Plasticized with Epoxidized Soybean Oil and Epoxidized Palm Oil

Yee Bond Tee,[a] Rosnita A. Talib,[b,c,*] Khalina Abdan,[d] Nyuk Ling Chin,[b] Roseliza Kadir Basha,[b] and Khairul Faezah Md Yunos [b]

To investigate epoxidized palm oil's (EPO) potential as plasticizer for poly(lactic acid) (PLA), its plasticizing effect was compared with commercialized epoxidized soybean oil (ESO). The plasticizers were respectively melt-compounded into PLA at 3, 5, 10, and 15 wt.%. As it was aimed for the blends to be characterized towards packaging appropriate for food products, they were hot-pressed into ~0.3-mm sheets, which is the approximate thickness of clamshell packaging. Fourier transform infrared spectroscopy (FTIR) confirmed the plasticizers' compatibility with PLA. At similar loadings, EPO was superior in reinforcing elongation at break (EAB), thermal, and barrier properties of PLA. The ductility of PLA was notably improved to 50.0% with addition of 3 wt.% of EPO. From thermogravimetric analysis (TGA), PLA/EPO5 improved PLA's thermal stability, while all PLA/ESO blends reported reduced thermal stability. From differential scanning calorimetry (DSC), the increase in crystallinity and the shifts in enthalpy of fusions in all plasticized blends denoted facilitation of PLA to form thermally stable α-form crystals. The addition of EPO enabled PLA to become highly impermeable to oxygen, which can extend its potential in packaging extensive range of oxygen sensitive food.

Keywords: Poly(lactic acid); Epoxidized oil; Plasticizer; Mechanical properties; Thermal properties; Barrier properties

Contact information: a: Department of Biotechnology, Faculty of Applied Sciences, UCSI University, 56000 Cheras, Kuala Lumpur, Malaysia; b: Department of Process and Food Engineering, Faculty of Engineering, Universiti Putra Malaysia, 43400 UPM Serdang, Selangor, Malaysia; c: Halal Products Research Institute, Universiti Putra Malaysia, 43400 UPM Serdang, Selangor, Malaysia; d: Institute of Tropical Forestry and Forest Products, Universiti Putra Malaysia, 43400 UPM Serdang, Selangor, Malaysia;
** Corresponding author: rosnita@upm.edu.my*

INTRODUCTION

Neat poly(lactic acid) (PLA) can be used for most rigid packaging applications. However in more extensive areas, especially in the manufacturing of flexible film, PLA is typically plasticized to widen its melt-processing ability, ductility, and impact properties (Murariu *et al.* 2008). Given the appropriate additives used, PLA can be competent in replacing petroleum-based polymers. For instance with additives to aid the form, fill, and seal (f/f/s) process, PLA has been productively used in Europe and US to replace polystyrene for yogurt containers (Mohan 2011a,b).

While petrochemical-based plasticizers such as phthalates can be added and are indeed critically important in plastic manufacturing especially in the PVC industry, their high toxicity, which impacts the health and environment, is a major setback (Groshar and

Okkerman 2000; Markarian 2007; Wang *et al.* 2013). For instance, the compounds butylbenzylphthalate (BBP), di-(2-ethylhexyl) phthalate (DEHP), and di-n-butylphthalate (DBP), which were mainly used as softener and plasticizer in toys, packaging materials, cosmetics, and in the PVC industry were identified as endocrine disruptors (Groshart and Okkerman, 2000; Markarian 2007).

Acknowledging the risks, efforts to find plasticizing compounds from natural resources have been escalating. Research on utilizing plant oils as plasticizers, including studies of rubber seed oil, neem oil, Madhuca oil, olive oil, corn oil, castor oil, soybean oil, and palm oil, have been picking up recently (Liu *et al.* 2006; Gamage *et al.* 2009; Xu and Qu 2009; Al-Mulla *et al.* 2010; Chua *et al.* 2012; Xiong *et al.* 2013). The benefits of these alternative plasticizers are definitely lower toxicity (Fenollar *et al.* 2009), good lubricity, lower volatility, (Lathi and Mattiason, 2007), low cost, renewable nature, and biodegradability (Wang *et al.* 2013).

In the present work, epoxidized soybean oil (ESO) and epoxidized palm oil (EPO) were compared as bio-sourced plasticizers for PLA. While ESO has long been established as one of the constituents for industrial production of PVC (HallStar 2007), EPO was more recently developed and studied as a potential plasticizer (Chieng *et al.* 2012; Silverajah *et al.* 2012; Al-Mulla *et al.* 2014; Tee *et al.* 2014). Our previous work reported positive results whereby EPO toughened and aided the melt-processing of PLA more readily than the commercially available ESO (Tee *et al.* 2014). The work continues with the comparison of ESO- and EPO-plasticized PLA on the basis of chemical, tensile, thermal, and barrier properties with the aim to present EPO as another sustainable plasticizer alternative to ESO appropriate for food packaging applications.

EXPERIMENTAL

Materials

Poly(lactic acid) resin (Ingeo 2003D, with MFI of 6 g/10 min at 210 ºC; D-lactide of 4 to 4.5%; and a bulk density of 0.85 g cm^{-3}) was purchased from NatureWorks LLC, USA. A chemically pure grade of epoxidized soybean oil (ESO) (Vikoflex® 7170, with average molecular weight of 1000 g mol^{-1}; minimum oxirane oxygen of 7.0 % and viscosity of 420.0 cP at 25 ºC) was provided by Arkema Inc., USA. Epoxidized palm oil (EPO) (with average molecular weight of 982 g mol^{-1}; minimum oxirane oxygen of 3.23 % and viscosity of 142.6 cP at 25 ºC) was provided by Advance Oleochemical Technology Division (AOTD), Malaysian Palm Oil Board (MPOB), Malaysia.

Preparation of Blends

The methodology for melt-compounding of 3, 5, 10, and 15 wt.% of ESO or EPO with PLA was also formerly reported (Tee *et al.* 2014). Prior to melt-blending, PLA resins were oven dried at 60 ºC overnight. PLA resins were premixed with ESO or EPO at loading of 3, 5, 10, and 15 wt.% of PLA and were melt-blended in an internal mixer (Brabender, Brabender Plastograph EC, Germany) at 170 ºC with a rotor speed of 50 rpm for 15 min. In view of preparing the blends potentially for food packaging applications, the blends were hot and cold pressed into ~0.3-mm sheets (which is the typical thickness of clamshell packaging) instead of 3-mm as was done formerly (Tee *et al.* 2014). They were pressed with a hot and cold press machine (Hot and Cold Press Machine, LP-50, Thailand) at 160 ºC for further characterization.

Fourier Transform Infrared Spectroscopy (FTIR)

The chemical compositions of ESO- and EPO-plasticized PLA were examined *via* FTIR (Perkin Elmer, Spectrum One FT-IR Spectrometer, US) with the attenuated total reflectance (ATR) technique. The spectra were recorded in absorbance mode with a resolution of 4 cm^{-1} in the range of 600 to 4000 cm^{-1}. Ten scans were averaged for each sample.

Tensile Test

Tensile tests were conducted in reference to ASTM D882. Seven rectangular strips with 100 mm × 15 mm × 0.3 mm dimensions were cut from each sample. Tensile strength, tensile modulus, and elongation at break were measured using a Universal Testing Machine (Instron®, Model 4301, US) with a load cell of 1 kN. The test was performed at a cross-head speed of 5 mm min^{-1} until tensile failure was detected. The average values of seven repetitions of each sample were reported with standard error.

Thermogravimetric Analysis (TGA)

PLA blends were subjected to thermal analysis using a thermogravimetric analyser (Perkin Elmer, TGA 7, US). Samples weighing 4 to 10 mg were placed in appropriate pans and heated from 30 to 600 ºC at 10 ºC min^{-1} under a nitrogen atmosphere at a flow rate of 20 mL min^{-1}.

The thermal stability of PLA resins, EPO, and ESO plasticizers during melt-compounding and hot-pressing was also analysed via TGA. They were heated in isothermal mode at 170 °C for 20 min under air at flow rate of 20 mL min^{-1}. PLA, PLA/EPO5, and PLA/ESO5 pallets were heated in isothermal mode at 160 °C for 20 min under air at flow rate of 20 mL min^{-1}.

Differential Scanning Calorimetry (DSC)

PLA blends were subjected to thermal analysis using a differential scanning calorimeter (Perkin Elmer, DSC 7, USA). Samples weighing 4 to 10 mg were placed in sample pans and sealed. They were then introduced into the heating cell of the DSC and heated from 30 to 200 ºC at 5 ºC min^{-1} under a nitrogen atmosphere at a flow rate of 10 mL min^{-1}.

Oxygen Permeability

The oxygen transmission rate (OTR) of a sample sheet was acquired in accordance with ASTM D3985-05 standard using an Oxygen Permeability Analyser (MOCON Inc., OpTech®-O_2 Platinum, US) at room temperature. A circular sample sheet with 110 mm diameter was prepared, and 50 cm^2 of the surface area was subjected to the test. Before testing, the sample sheet was sealed with a silicone ring coated with high vacuum grease within the diffusion chamber. One side of the sheet (test cell at the lower half of the chamber) was purged with pure nitrogen at flow rate of 10 mL min^{-1} until 0% of O_2 was confirmed. Then, pure oxygen (99.9%) was continuously purged on the upper half of the chamber with barometric pressure of 760 mmHg (or 101,325 Pa). The test was stopped when at least three consecutive transmission rate readings differed by less than 5% were reported whereby an equilibrium state was presumed to have been reached. Oxygen permeability (*OP*) was calculated using Eq. 1 where ΔP_{O2} was taken as 101,325 Pa as the

O_2 pressure on the N_2 side of the sheet was assumed to be zero (Ayranci and Tunc 2003). The average values three repetitions of each sample were reported with standard error,

$$OP = \frac{OTR\ x}{\Delta P_{O2}} \quad (1)$$

where *OP* is the oxygen permeability [m^3 m m^{-2} s^{-1} Pa^{-1}]; *OTR* is the oxygen transmission rate [mL m^{-2} day^{-1}]; ΔP_{O2} is the oxygen pressure difference across the sheet [Pa]; and *x* is the thickness of sheet [m].

Water Vapour Permeability

The water vapour transmission rate (WVTR) of a sample sheet was acquired in accordance to ASTM F1249-06 using Water Vapour Permeability Analyser (Permatran W3/31, MOCON Inc., US). A circular sample sheet with 110 mm diameter was prepared, and 50 cm^2 of the surface area was subjected to the test. Before testing, the sheet was sealed with a silicone ring coated with high vacuum grease within the diffusion chamber. The tests were run at 37.8 ^oC with 90 ± 2% RH at the permeant side, and 0 ± 2% RH at the test cell, and the tests were stopped when at least three consecutive transmission rate readings differed by less than 5% and were reported where an equilibrium state was presumed reached. Water vapour permeability (WVP) was calculated using Eq. 2 whereby the water vapour pressure, P_w at 37.8 ^oC was 6545 Pa (Carvalho and Grosso 2004; Cao *et al.* 2009). The calculated average values of three repetitions of each sample were reported with standard error,

$$WVP = \frac{WVTR\ x}{P_w(RH_1 - RH_2)} \quad (2)$$

where WVP is the water vapour permeability [kg m m^{-2} s^{-1} Pa^{-1}]; WVTR is the water vapour transmission rate [g m^{-2} day^{-1}]; P_w is the water vapour pressure at temperature during the experiment [Pa]; *x* is the thickness of sheet [m]; and RH_1-RH_2 is the relative humidity gradient used in the experiment.

Morphology Characterization

The morphologies of tensile fracture surface of sample sheet were observed using a variable pressure scanning electron microscope (LEO, 1455VPSEM, England) at an accelerated voltage of 20 kV. Before scanning, the samples were sputter-coated with gold.

RESULTS AND DISCUSSION

FTIR Spectra

The FTIR spectra of EPO and ESO plasticizers were compared as shown in Fig. 1. Both had similar prominent characteristic peaks, which correspond to the ester sites and epoxy groups (also known as oxirane rings) (C-O-C) in epoxidized oil. Both spectra displayed a peak at 1743 cm^{-1}, which correspond to the aliphatic -C=O stretching of esters (Adhvaryu and Erhan 2002; Al-Mulla *et al.* 2010; Silverajah *et al.* 2012). The peak at 1250 cm^{-1}, and small intensity vibrations around 950 to 850 cm^{-1}, were indicative of C-O-C

stretching from oxirane vibrations (Téllez *et al.* 2009; Al-Mulla *et al.* 2014). In addition, the peak at 1250 cm^{-1} also overlays with another compound, mostly C-O ester in oil (Téllez *et al.* 2009). The strong peaks at 2929 cm^{-1} and 2856 cm^{-1} were from the stretching vibrations of $-CH_2$ (Al-Mulla *et al.* 2014; 2010; Silverajah *et al.* 2012).

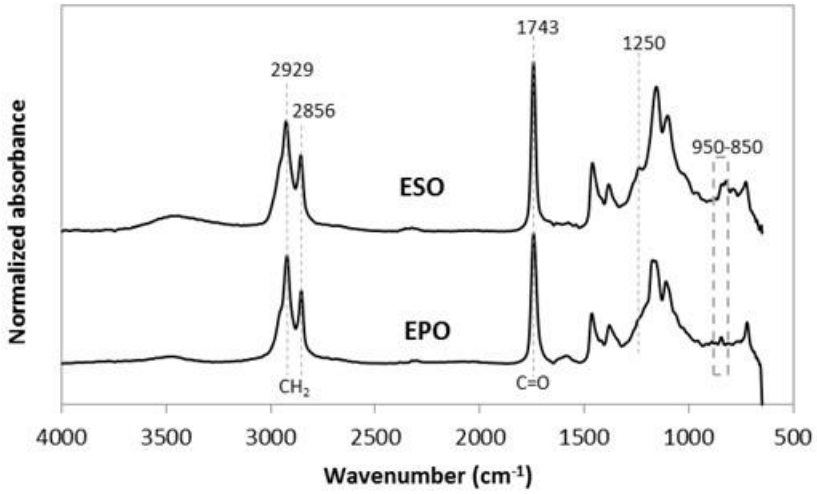

Fig. 1. Normalized absorbance as a function of wavenumber (cm^{-1}) for EPO and ESO in the FTIR region from 600 to 4000 cm^{-1}

Upon validating the epoxidization of these triglycerides, they were respectively added at various loadings in PLA. Their FTIR spectra were as shown in Figs. 2 and 3. The stretching vibrations of CH_2 and C=O in PLA were at 2926, 2852, and 1754 cm^{-1}. As for the plasticizers, they were slightly different at 2929, 2856, and 1743 cm^{-1}. Upon blending the plasticizers into PLA, these peaks were neutralized at 2927, 2855, and 1746 cm^{-1}, which may indicate some intramolecular interactions and compatibility between the plasticizers and PLA.

Changes in the intensity of these peaks were also observed. All ESO- and EPO-plasticized PLA had increased peak intensity corresponding to C=O stretching (at 1746 cm^{-1}) as compared to that of neat PLA's (1754 cm^{-1}). The increase in the stretching vibrations of CH_2 (2927 and 2855 cm^{-1}) was more noticeable at high EPO (10 wt.% and above) and ESO (15 wt.%) content. In addition, the disappearance of stretching vibrations at 1250 cm^{-1} and around 950 to 850 cm^{-1} (from the epoxy groups) may also indicate the possible interaction between the plasticizers and PLA (Téllez *et al.* 2009; Silverajah *et al.* 2012).

It is typical to accept that there was no interaction between a plasticizer and a thermoplastic when the FTIR spectra remained unchanged upon addition (Maizatul *et al.* 2013), while a minute shift or peak intensity change can provide evidence of possible interaction between the materials (Al-Mulla *et al.* 2014; 2010; Silverajah *et al.* 2012; Zakaria *et al.* 2013).

FTIR spectra of PLA/EPO blends were also reported by Al-Mulla *et al.* (2010) and Silverajah *et al.* (2012) with similar findings. With schematic diagram of interaction provided, the compatibility and interaction between PLA and epoxidized plant oils was proposed to be from the hydrogen bonding between terminal hydroxyl groups of PLA and the oxirane groups of the EPO (Al-Mulla *et al.* 2010) and ESO (Xu and Qu 2009).

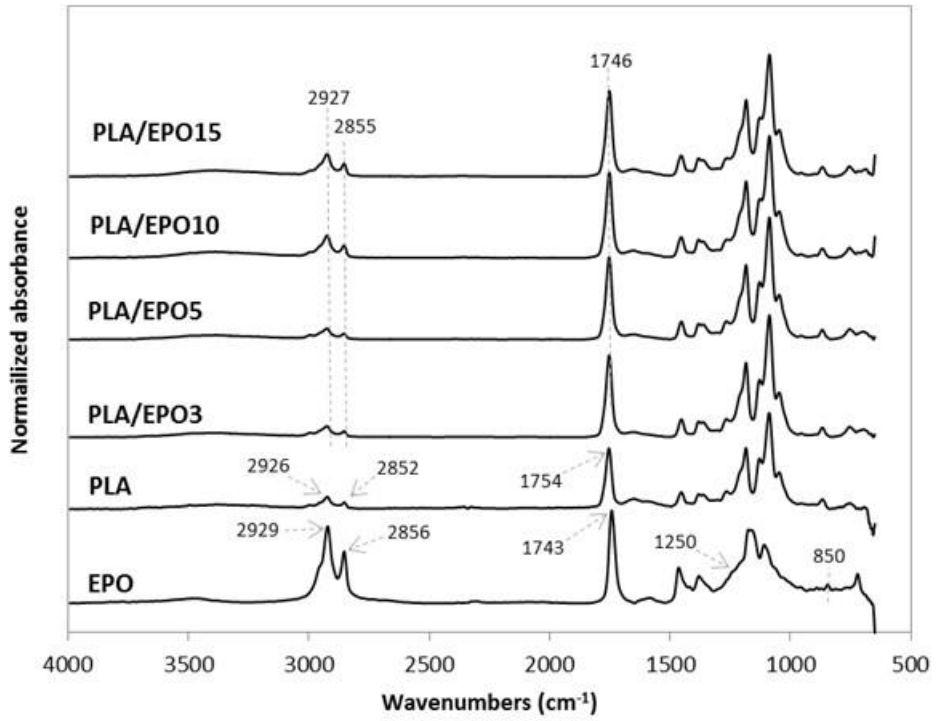

Fig. 2. Normalized absorbance as a function of wavenumber (cm^{-1}) for EPO, PLA, and PLA/EPO at various EPO concentrations in the FTIR region from 600 to 4000 cm^{-1}

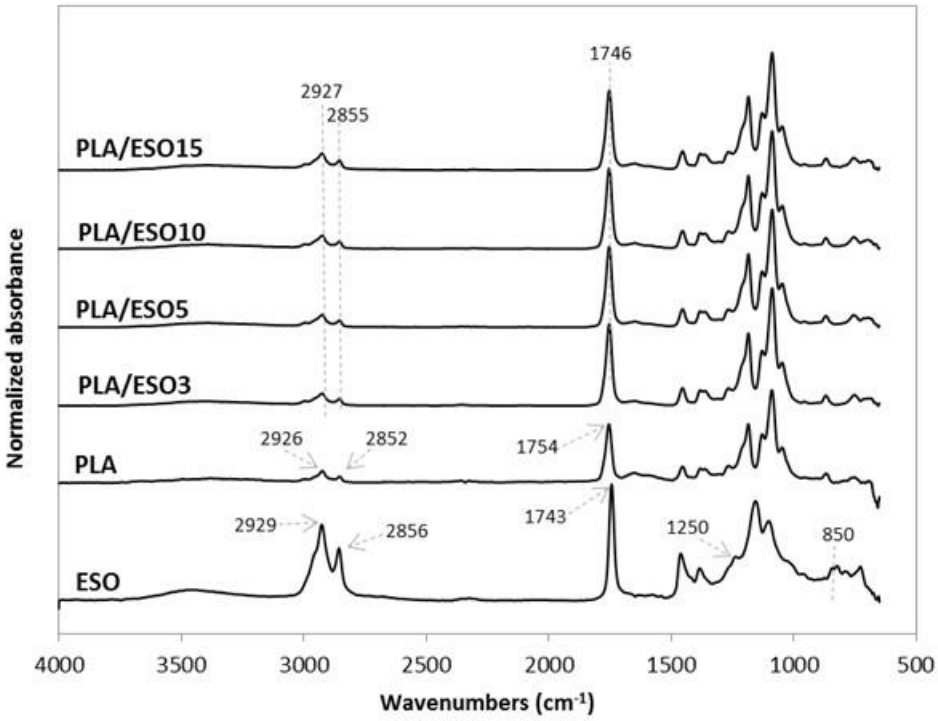

Fig. 3. Normalized absorbance as a function of wavenumber (cm^{-1}) for ESO, PLA, and PLA/ESO at various ESO concentrations in the FTIR region from 600 to 4000 cm^{-1}

Tensile Properties

For comparison, the trend with tensile strength, modulus, and elongation at break at increasing EPO and ESO loadings in PLA were respectively plotted as shown in Figs. 4 to 6. As shown in Fig. 4, both EPO and ESO caused gradual decrease in tensile strength of PLA as the loading increased. In the case of EPO the tensile strength values decreased to a greater extent. At low loading of 3 and 5 wt.% of ESO, statistically there were no significant differences in tensile strength as compared to PLA. As for the higher loading of ESO and all loadings of EPO, their addition into PLA caused significant decrease in tensile strength of PLA at 47 MPa, to the lowest at 28 MPa for PLA/ESO15, and 30 MPa for PLA/EPO15.

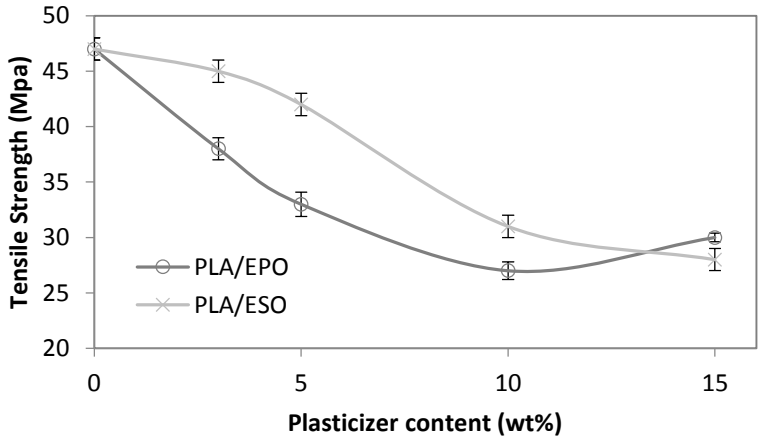

Fig. 4. Tensile strength (MPa) of plasticized PLA at various EPO and ESO wt.%

As shown in Fig. 5, PLA with tensile modulus of 7 GPa was significantly reduced and remained constant at 3 to 4 GPa despite increasing the loading of added respective plasticizers. The drop in tensile modulus indicated an increase in samples' flexibility. Correspondingly, an apparent increase in elongation at break was reported. From Fig. 6, the increase in elongation at break or ductility of ESO-plasticized PLA at increasing ESO loading was exponential. At low loading of 3 and 5 wt.%, the increases in elongation at break were little, and these findings were consistent with the insignificant decrease in tensile strength. As ESO loading increased up to 15 wt.%, the blend turned ductile with elongation at break of 68.6%. Nevertheless, it should be noted that a marked standard error at ±15.79 was also reported. Comparatively, EPO was superior in improving the ductility of PLA for all loadings tested. Even at 3 wt.%, PLA/EPO3 exhibited approximately 16 times higher elongation at break (50.0%) as compared to PLA/ESO3's (3.1%). That aside, comparable elongation at break with PLA/ESO15 was achieved with addition of only 5 wt.% of EPO in PLA with a noticeably lower standard error (68.2% (± 6.41)). The change in elasticity upon addition of both plasticizers in PLA samples can be observed in Fig. 7 (b) and (c), where the tensile deformed strips exhibited stress whitening and appeared more elongated as compared to the rigid PLA strip (Fig. 7 (a)). This was due to the enhanced straining of craze fibrils from the local plasticization of ESO- and EPO-rich phases within the matrix.

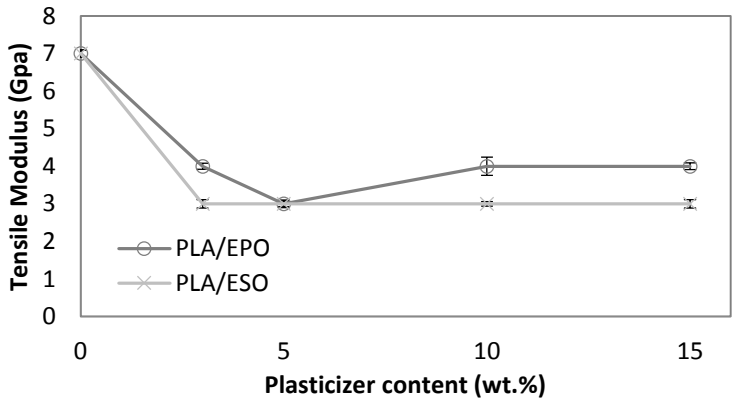

Fig. 5. Tensile modulus (GPa) of plasticized PLA at various EPO and ESO wt.%

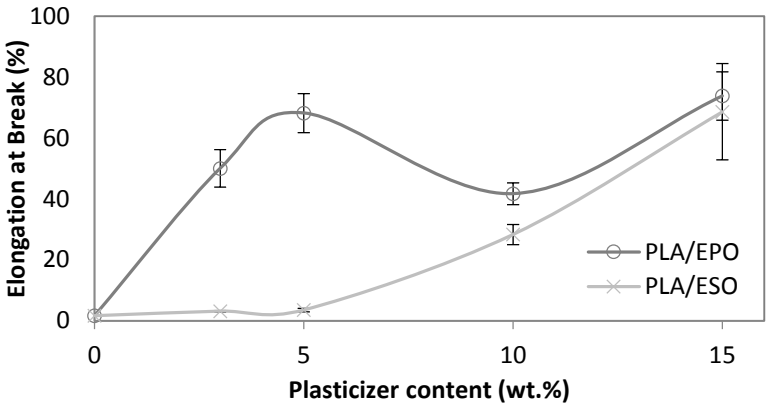

Fig. 6. Elongation at Break (%) of plasticized PLA at various EPO and ESO wt.%

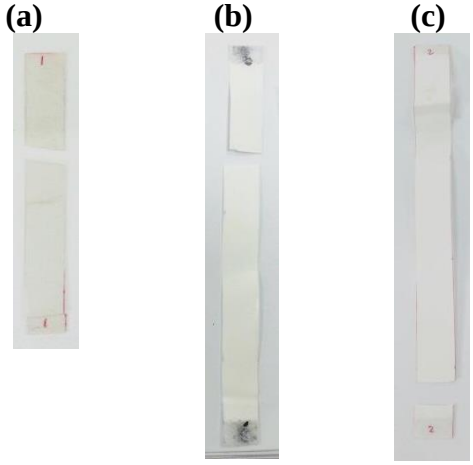

Fig. 7. Post tensile deformed strips of (a) PLA; (b) PLA/EPO5; and (c) PLA/ESO15

It is typical that the increase of elongation at break (and impact resistance) of a plasticized thermoplastic was complemented with a reduction in tensile strength and modulus as they softened and became more flexible. Such occurrence can be explained based on several widely accepted mechanisms of plasticization, namely the lubricity, gelation, and the free volume theory (Mekonnen *et al.* 2013). The reduction in tensile strength and rigidity of PLA from the increasing loading of ESO and EPO respectively can

be explained *via* gelation theory, where their presence weakened the polymer gel structure, which also improved PLA's flexibility. These low molecular weight plasticizer molecules disrupted and reduced the polymer-polymer interactions (such as hydrogen bonds, ionic forces, or van der Waals), which hold the polymer chains together (Mekonnen *et al.* 2013; Xu and Qu 2009). When the loading of plasticizer was increased, more polymer-polymer connection points were dissolved, which eventually weakened the attractive forces between the polymer chains and reduced the tensile strength. At all loadings tested, EPO was significantly superior to ESO in increasing the ductility of PLA. This correlated well with the morphology results where the dispersion of plasticizer microdroplets within polymer matrix may be desirable for plasticization. As ESO up to 5 wt.% was added into PLA, there was a minimal change in tensile strength and elongation at break. This may be due to the non-presence of ESO-rich phases (microdroplets) within the matrix (from the possibly better miscibility with PLA as discussed in the morphology analysis). Still, the significant reduction in tensile modulus denoted the presence of ESO within the polymer. At this loading of ESO, the plasticization effect can be explained with the lubricity and gel theories. Although comparatively insignificant to EPO, the dissolved ESO within the polymer chains could have still acted as lubricant in reducing friction, which improved its plastic deformation by promoting the polymer chain mobility to slide past one another (Ghosh *et al.* 2010; Silverajah *et al.* 2012; Mekonnen *et al.* 2013). As for EPO and higher loading of ESO, the dispersion of microdroplets within the matrix resulted in enhanced elongation at break, at least 27 times higher as compared to neat PLA. The accumulation of plasticizer rich phases increased the free volume within the rigid PLA. From this theory, it was stated that the free volume provided an internal space for the movement of polymer chains (Mekonnen *et al.* 2013). The dispersed microdroplets of plasticizers within the PLA matrix clearly provided more free volume, which eventually improved PLA's flexibility. Researchers have reported similar trends and stated that these scattered plasticizer microdroplets provided local plasticization, which promoted the formation of whitened and elongated craze fibrils (Kulinski and Piorkowska 2005; Piorkowska *et al.* 2006; Ali *et al.* 2009). Ali and co-workers (2009) reported a similar observation as the present PLA/ESO blend showed significant improvement in PLA's ductility that was enabled when 10 wt.% of ESO was added.

Thermogravimetric Analysis

To examine the possible loss of plasticizers, thermally, from the present melt-compounding, TGA isothermal curves were studied at 170 °C, as shown in Fig. 8. Within 15 min (which is the time for melt-compounding), 99.9% of both of the plasticizers remained. It is therefore accepted that both plasticizers had comparable thermal stability with no weight loss due to evaporation within the present melt-compounding parameters. PLA resins had remains of 99.8%, whereby the weight loss was considered as negligible.

Figure 9 shows the TGA isothermal curves of PLA and plasticized PLA pellets at 160 °C. This test was done to study the influence of plasticizers on the thermal stability of PLA during the hot-pressing procedure at 160 °C. Of all the blends tested, PLA/ESO5 showed the least thermal stability, which equilibrated at 97.0% of the remaining weight. Within the actual hot-pressing time (which was slightly more than 8 min), PLA/ESO5 exhibited a total weight loss of 2.5%. Differently, adding similar loading of EPO into PLA resulted in negligible weight loss of 0.3%. This showed that EPO-plasticized PLA were more thermally stable than those with ESO.

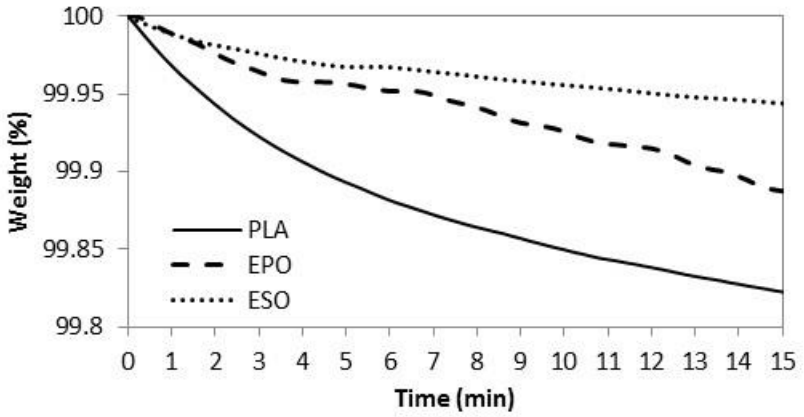

Fig. 8. TGA curves for raw materials at 170 °C

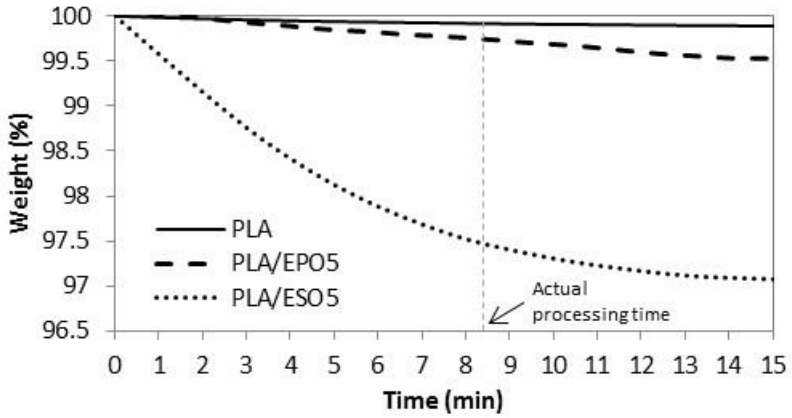

Fig. 9. TGA curves for post-mixed pallets at 160 °C

The TGA and DTG curves of hot-pressed samples were grouped accordingly, whereby Figs. 10 and 11 show the TGA and DTG curves of various proportional contributions of PLA/EPO. Figures 12 and 13 show the TGA and DTG curves of various proportions of PLA/ESO. Focusing at the thermogravimetric behaviour of EPO- and ESO-plasticized PLA, all revealed only one major mass loss step.

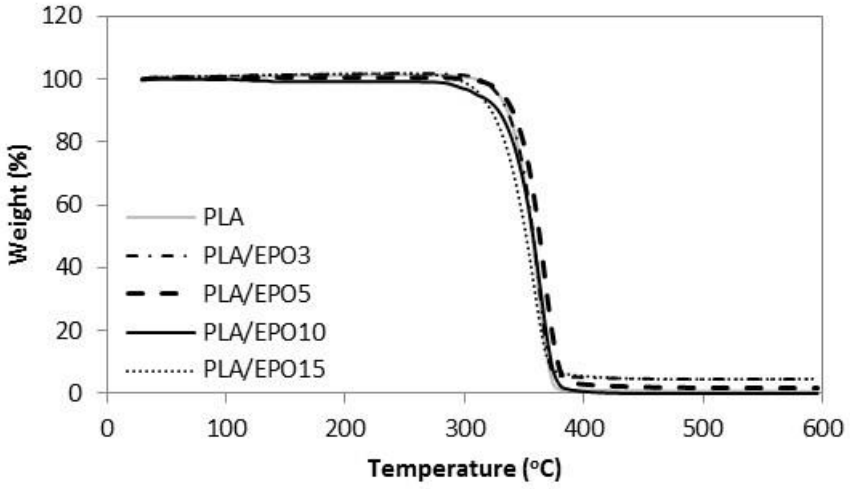

Fig. 10. TGA curves for PLA and PLA/EPO at various EPO loadings

For ease of comparison, the onset of degradation temperature T_o, maximum degradation temperature T_{peak}, and the end of degradation temperature T_e of neat and plasticized PLA are tabulated in Table 1. Of all the plasticized blends, PLA/EPO5 (with T_o at 298 °C and T_{peak} at 368 °C) was the only sample with improved thermal stability as compared to that of neat PLA's (with T_o at 275 °C and T_{peak} at 365 °C). Nevertheless, considering the onset of thermal degradation, the addition of EPO up to 10 wt.% maintained the T_o of PLA at 275 °C. The addition of 15 wt.% of EPO in PLA became excessive and this significantly decreased its T_o and T_{peak}. Differently for PLA/ESO blends, the increase of ESO in PLA gradually decreased its thermal stability. PLA/ESO15 reported the lowest thermal stability of all blends. In general, PLA/EPO blends were more thermally stable as compared to PLA/ESO blends with PLA/EPO5 being the optimum concentration to reinforce the thermal stability of PLA.

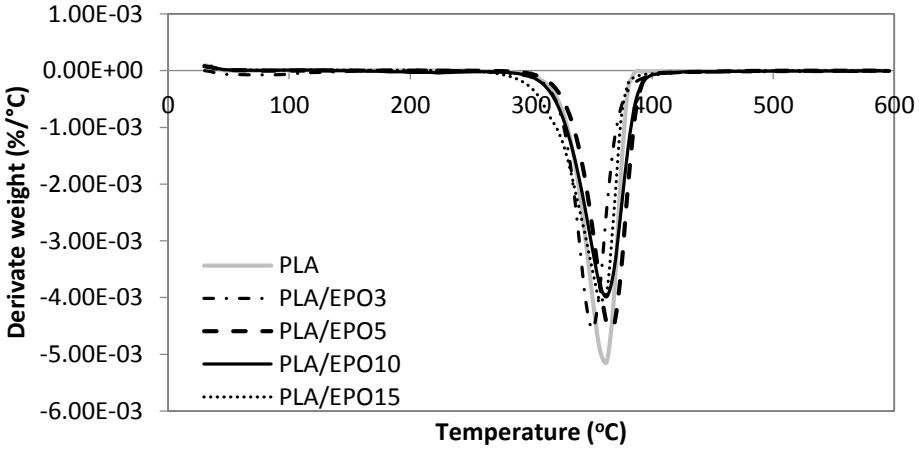

Fig. 11. DTG curves for PLA and PLA/EPO at various EPO loadings

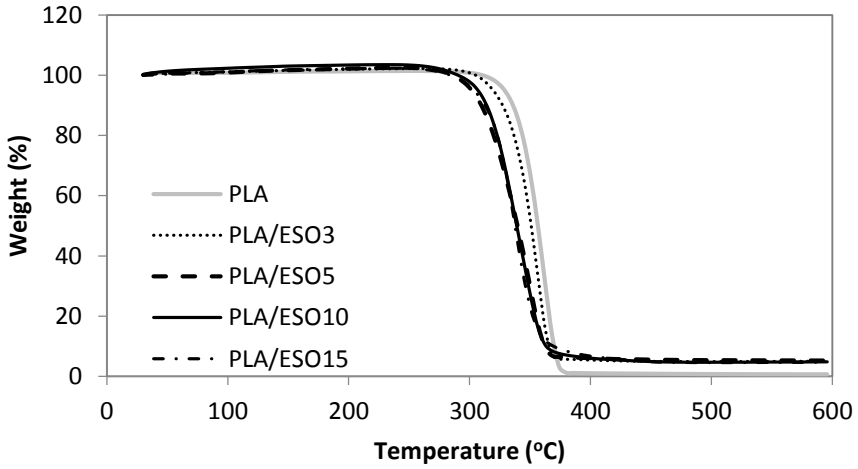

Fig. 12. TGA curves for PLA and PLA/ESO at various EPO loadings

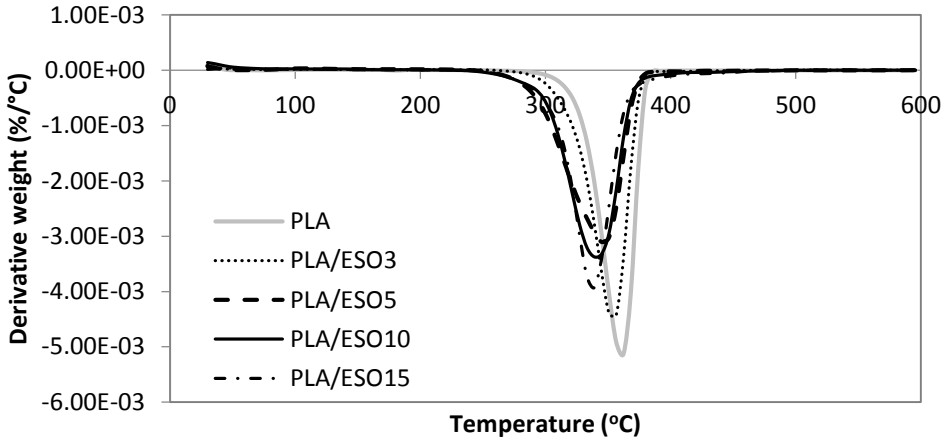

Fig. 13. DTG curves for PLA and PLA/ESO at various EPO loadings

Table 1. TGA and DTG Results for PLA and PLA Plasticized with EPO and ESO at Various Loadings

Sample	TGA and DTG parameters		
	T_o, (°C)	T_{peak}, (°C)	T_e, (°C)
PLA	275	363	378
PLA/EPO3	275	351	403
PLA/EPO5	298	368	409
PLA/EPO10	275	363	409
PLA/EPO15	258	357	398
PLA/ESO3	263	357	392
PLA/ESO5	240	345	392
PLA/ESO10	234	342	398
PLA/ESO15	234	339	398

Researchers have reported a decrease in polymer's thermal stability resulting from the addition of various plasticizers, and many have proposed that the decrease was from the vaporization of the plasticizers (Arrieta *et al.* 2013, 2014; Burgos *et al.* 2013; Jia *et al.* 2014; Masirek *et al.* 2007; Murariu *et al.* 2008). To investigate whether the reduction of thermal stability of plasticized PLA was due to the volatility of EPO and ESO respectively, thermogravimetric analyses on the plasticizers were done. EPO reportedly degrade in the range of 287 to 491 °C, with degradation peak at 409 °C, while ESO had slightly lower thermal stability with degradation range of 287 to 485 °C, and degradation peak at 392 °C. Both of these bio-sourced plasticizers had higher degradation temperatures than that of PLA's, and thus the decrease in thermal stability of the plasticized PLA blends was not due to the vaporization of these plasticizers. Still, the higher degradation temperature of EPO itself, as compared to that of ESO's, resulted in higher thermal stability of all PLA/EPO blends than that of PLA/ESO blends. This explanation can equally account for the observed minimum in the weight loss during thermal processing. Silverajah *et al.* (2012) subjected PLA plasticized with 1 and 5 wt.% of EPO to TGA tests, and similar to PLA/EPO5 in the present work, they reported higher T_o and T_{peak} as compared to that of PLA's. From the present work, an optimum EPO concentration in PLA could be achieved at 5 wt.%, where a homogeneous blend with good interaction within the blend occurred. It was also reported elsewhere that an increase in thermal stability of plasticized PLA was due to the good plasticizer dispersion and their interaction with PLA matrix (Silverajah *et al.* 2012; Burgos

et al. 2013). In addition, the homogeneously dispersed EPO could have acted as a protective barrier, which deterred the release of volatile degradation products out from the blend and therefore delayed the degradation (Silverajah *et al.* 2012; Burgos *et al.* 2013; Al-Mulla *et al.* 2014). It is worth noting that the lowest T_o recorded at 234 °C (in PLA/ESO blends) was still acceptable, as it was higher than those used in food processing or distribution, confirming their thermal stability with no apparent weight loss after processing (Arrieta *et al.* 2014).

Differential Scanning Calorimetry Analysis

Figure 14 shows the DSC curves of PLA plasticized with various concentrations of respective plasticizers, and Table 2 lists the glass transition temperature T_g, crystallization temperature T_c, melting temperature T_m, enthalpy of crystallization ΔH_c, enthalpy of fusion ΔH_m, and degree of crystallinity X_c from DSC tests. T_g was reported as the onset temperature of glass transition, while T_c and T_m were reported as the peak maxima. The degree of crystallinity was calculated using $X_c = \Delta H_c / 93$, with 93 J g^{-1} as the melting enthalpy of a PLA crystal of infinite size (Cao *et al.* 2003; Fischer *et al.* 1973).

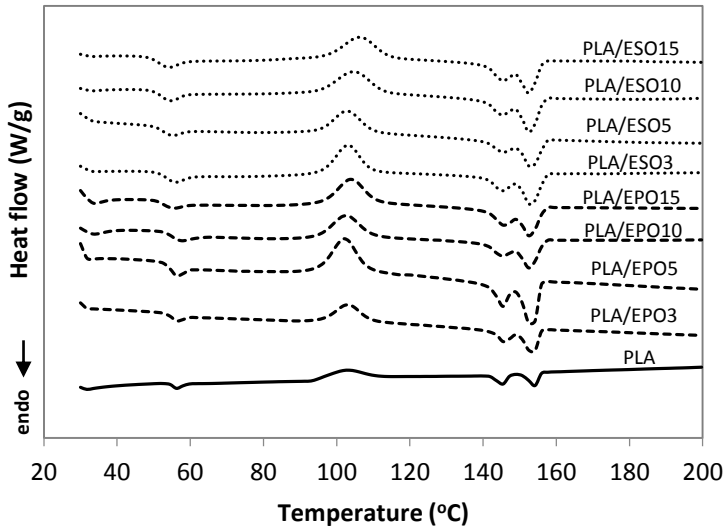

Fig. 14. DSC curves for PLA and PLA plasticized with EPO and ESO at various loadings

Table 2. DSC Results for PLA and PLA Plasticized with EPO and ESO at Various Loadings

Sample	T_g, (°C)	T_c, (°C)	T_{m1}, (°C)	T_{m2}, (°C)	ΔH_{m1}, (J g^{-1})	ΔH_{m2}, (J g^{-1})	ΔH_c, (J g^{-1})	X_c, (%)
PLA	54	102	146	154	3.1	3.7	8.2	9
PLA/EPO3	54	103	146	153	2.9	7.3	14.8	16
PLA/EPO5	53	102	145	153	5.5	15.3	31	33
PLA/EPO10	53	103	145	153	3.0	9.0	22.2	24
PLA/EPO15	51	104	145	153	3.4	8.8	22.7	24
PLA/ESO3	51	103	145	153	3.6	11.1	24.4	26
PLA/ESO5	51	103	145	153	2.3	9.9	20.3	22
PLA/ESO10	50	105	145	153	3.6	11.7	21.7	23
PLA/ESO15	49	106	145	153	3.8	9.9	21.7	23

The incorporation of plasticizers at various loadings did not result in any new peak or major shift of the existing peaks (T_g, T_c, T_{m1}, and T_{m2}). There was no occurrence of two separated T_g values in the plasticized blends, which indicated that the plasticizers were not immiscible with PLA. With similar loading of plasticizers incorporated, ESO was able to influence the T_g and T_c of PLA more readily than EPO, which also signify better miscibility of ESO as compared to EPO. The T_g value of PLA was reduced to 51 °C upon addition of 3 wt.% of ESO, while comparable T_g was attained with 15 wt.% of EPO added. The T_g was gradually reduced with the increasing of ESO loading, and the lowest T_g was reported at 49 °C for PLA/ESO15.

As has been discussed in regards to tensile properties, the addition of a plasticizer enhanced the segmental mobility of polymer chains. From the thermal aspect, this also reduces T_g and promotes crystallizability, meaning an increase in X_c and typically a reduction in T_c (Kulinski *et al.* 2006; Martin and Avérous 2001; Pillin *et al.* 2006). However in the present work, the decrease in PLA's T_g from the addition of EPO and ESO plasticizers were low, with maximum reduction of 3 °C and 5 °C respectively as compared to other incorporation of plasticizers such as PEG (Arrieta *et al.* 2014; Kulinski and Piorkowska 2005; Masirek *et al.* 2007; Pillin *et al.* 2006), acetyl(tributyl citrate) (ATBC) (Arrieta *et al.* 2014), dioctyl phthalate (DOP) (Yang *et al.* 2009), bis(2-ethylhexyl) adipate (DOA) (Murariu *et al.* 2008), poly(1,3-butanediol) (PBOH) (Pillin *et al.* 2006), acetyl glycerol monolaurate (AGM) (Pillin *et al.* 2006), and dibutyl sebacate (DBS) (Pillin *et al.* 2006). DSC analysis of PLA/ESO and PLA/EPO blends from the present work was compared with the published works using similar materials and they also reported minor reduction in T_g (Ali *et al.* 2009; Dai *et al.* 2014; Silverajah *et al.* 2012). In addition to no evidence of two separated glass transition temperatures, this denoted that they were both partially-miscible with PLA- with ESO having better miscibility with PLA due to the higher extend of T_g reduction. This correlated well with the morphology analysis where phase separation of ESO occurred at higher content as compared to EPO. It is the phase separation that caused the insignificant reduction in T_g in the present work. Similarly, Yang *et al*. (2009) and Kulinski *et al*. (2006) reported minor decrease of T_g when the plasticizers DOP and poly (propylene glycol) (PPG) loading reached a certain amount where phase separation within PLA matrix occurred.

The crystallization behavior remained almost unaffected for both plasticizers content up to 10 wt.% as opposed to the typical reduction in T_c. A more apparent change in T_c occurred only at higher plasticizer concentrations. ESO and EPO facilitated the growth of crystallites where the highest X_c at 26% was reported by PLA/ESO3 and 33% was reported for PLA/EPO5. The continued increase of plasticizers loading in the blend reduced the X_c as plasticizer droplets were accumulated into separate phases. The varying X_c of the plasticized blends in the present work could be due to presence of the varying amount of additional hydrogen bond linkages (from EPO and ESO), which altered the alignment of the polymer chains (Silverajah *et al.* 2012; Wang *et al.* 2008).

As for the melting behaviour, the addition of both plasticizers at various loadings did not cause major changes in the T_{m1} and T_{m2} of the semicrystalline PLA. Several authors reported a similar trend (Ali *et al.* 2009; Dai *et al.* 2014; Silverajah *et al.* 2012). Nevertheless, there was a shift in ΔH_{m1} and ΔH_{m2}, whereby ΔH_{m2} of all plasticized PLA blends were significantly steeper as compared to that of neat PLA. Based on the melt-recrystallization behaviour of semicrystalline polymer, this indicated that both plasticizers can and were comparable in facilitating PLA to form more thermally stable α-form crystals

than δ-form crystals without affecting PLA's melting points (Wasanasuk and Tashiro 2011).

Barrier Properties

Table 3 lists the OTR, WVTR, OP, and WVP of PLA plasticized with various concentrations of respective plasticizers. The transmission rates and permeabilities can be reported interchangeably, as both have been typically used in the literature for discussion of barrier properties. As evaluation, comparatively larger permeability values or transmission rates were attributed to poorer barrier behaviors; and comparatively smaller permeability values or transmission rates were attributed to a better barrier.

Table 3. OTR, OP, WVTR, and WVP of PLA and PLA Plasticized with EPO and ESO at Various Loadings

Sample	Thickness of sample (mm)	OTR (mL m^{-2} day^{-1})	OP (x10^{-17} m^3 m m^{-2} s^{-1} Pa^{-1})	WVTR (g m^{-2} day^{-1})	WVP (x10^{-17} kg m m^{-2} s^{-1} Pa^{-1})
PLA	0.35 (±0.02)	1542.5 (±1.1)	6.2	5.6 (±0.0)	3.9
PLA/EPO3	0.38 (±0.00)	N.D.	N.D.	7.3 (±0.2)	5.5
PLA/EPO5	0.38 (±0.00)	N.D.	N.D.	7.0 (±0.1)	5.2
PLA/EPO10	0.38 (±0.00)	N.D.	N.D.	7.4 (±0.0)	5.5
PLA/EPO15	0.35 (±0.02)	576.8 (±0.7)	2.3	8.3 (±0.1)	5.7
PLA/ESO3	0.37 (±0.01)	748.6 (±2.5)	3.2	6.6 (±0.1)	4.8
PLA/ESO5	0.36 (±0.01)	642.3 (±0.2)	2.6	8.2 (±0.2)	5.8
PLA/ESO10	0.36 (±0.01)	462.6 (±0.4)	1.9	8.7 (±0.2)	6.2
PLA/ESO15	0.35 (±0.02)	458.3 (±1.5)	1.8	12.5 (±0.1)	8.6

Values are given as average (± standard error).
N.D. is equivalent to non-detectable; where the OTR value was below the detection limit of 0.0001 mL day^{-1} and oxygen content of 0.001%.

The addition of EPO and ESO in PLA significantly increased PLA's oxygen barrier capability, where at least 50% of reduction in OTR or OP was found. Comparatively, EPO was more effective in improving PLA's oxygen barrier, whereas oxygen transfer was not detectable by the instrument after the addition of EPO up to 10 wt.%. An increase in OTR was recorded when EPO loading further increased to 15 wt.%. Nevertheless, PLA/EPO15 had a medium oxygen barrier with OTR that was still (270%) lower than that of neat PLA's. As for PLA that was plasticized with ESO, despite not achieving an entirely impermeable state, all PLA/ESO blends shifted the medium-low oxygen barrier of PLA sheet to medium range (11 to 1000 mL m^{-2} per day) (Abdellatief and Welt 2012). With at least twice the improvement, the oxygen barrier gradually increased as the ESO loading increased up to 15 wt.%.

Dissimilar to the trend in oxygen barrier, the addition of both plasticizers in PLA respectively reduced the water vapour barrier capability of PLA. Both plasticizers resulted in a gradual increase in WVTR as their loading was increased from 3 to 15 wt.%, with PLA/EPO blends recorded WVTR in the range of 7.0 to 8.3 g m^{-2} per day while PLA/ESO blends gave rise to a wider range of 6.8 to 12.5 g m^{-2} per day.

Generally, the addition of EPO and ESO plasticizers into PLA increased oxygen barrier but reduced water vapour barrier. Permeability is the product of and directly proportional to solubility (*S*), and diffusion coefficients (*D*) of permeating molecule, $P = D.S$ (Figura and Teixeira 2007). The diffusion coefficient was dependent on the polymer

structure, which includes its tortuosity and free volume, while the solubility coefficient was dependent on the permeant's solubility on a molecular scale (Courgneau *et al.* 2011). The epoxidized oils are not water-soluble. Therefore, the increase in WVP was mainly due the diffusivity of water vapour molecules rather than their solubility. The localized plasticizers within the matrix increased the polymer chains mobility and free volume, which widened the interstitial space and thus eased the diffusion of water molecules through the PLA sheet (Bourtoom 2008; Laboulfie *et al.* 2013). A quick validation can be done by comparing the WVTR (or WVP) and morphology analysis between PLA/EPO3 and PLA/ESO3. Notable microdroplets of EPO were seen dispersed within the matrix of PLA/EPO3 from the morphology analysis, while it was absent in PLA/ESO3; despite similar plasticizer loading used. This may correlate with the higher WVTR (or WVP) of PLA/EPO3 sheet as compared to that of PLA/ESO3, where the higher content of free volume in PLA/EPO3 created more pathways for water vapour diffusion.

A contradicting drop in OP (or OTR) was reported in the present work with the addition of both epoxidized oils. The drop was so significant that an absolute oxygen barrier in most of the PLA/EPO blends was achieved, despite repeated examinations. Addition of both EPO and ESO can extend the potential of PLA in packaging for a wider range of oxygen sensitive food products. Especially for PLA/EPO blends with comparatively better barrier properties, their potential may extend to products such as processed meat packaging (with OTR and WVTR requirement of 3.1 to 15.5 mL m^{-2} per day and 3.1 to 7.75 g m^{-2} per day) and cheese (with OTR and WVTR requirement of 9.3 to 15.5 mL m^{-2} per day and 1-15.5 g m^{-2} per day) (Butler and Morris 2013). Similarly, Srinivasa and co-workers (2007) also reported an opposing trend of an increase in water vapour permeability with a drastic decrease in oxygen permeability upon plasticizing chitosan films with PEG and fatty acids. While the increased crystallinity of all plasticized PLA could have caused restriction to the gas permeation, it was not the only factor. The trend of crystallinity increasing from the DSC analysis did not entirely agree with that of OTR of plasticized PLA. The excellent oxygen barrier of the epoxidized oils could have offset the anticipated reduction in the O_2 transmission through PLA from the increased free volume. The lipids could have packed into the micro-channels or pores of matrix and obstructed the movement of the gas molecules (Srinivasa *et al.* 2007). Plasticizing PLA would have prevented cracks and pores formation on PLA's surface, which eventually reduces the channels for gas molecules transmission (García *et al.* 2000).

Morphology Characterization

Figure 15 shows the micrographs of tensile fracture surfaces of PLA/EPO and PLA/ESO sheets at various plasticizer loadings. In all blends of plasticized PLA, there were fibrillations of matrix, or web-like structures of strained matrix, which was not seen in neat PLA. Figure 16 shows a clearer observation on the improved ductility in plasticized-PLA. Dense arrays of whitened fibrils known as craze, were seen at the fracture surface due to straining from tensile test. The crazes were mostly perpendicular to the applied stress and were inter-dispersed with elongated microvoids.

From the tensile fracture surfaces of all PLA/EPO blends, microvoids were seen scattered within the matrix. These microvoids, with centres appearing darker than the matrix, were from the retention of EPO micro-droplets, which were partially removed from the matrix as it was fractured. At 3 wt.% of EPO in PLA, about 1 µm microvoids were evenly dispersed within the matrix. As EPO loading increased to 10 wt.% and 15 wt.%, the size of the microvoids deviated significantly with more discernible EPO rich phases.

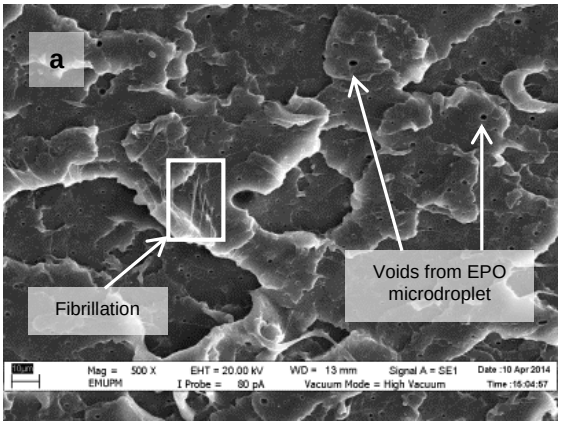
a
Fibrillation
Voids from EPO microdroplet

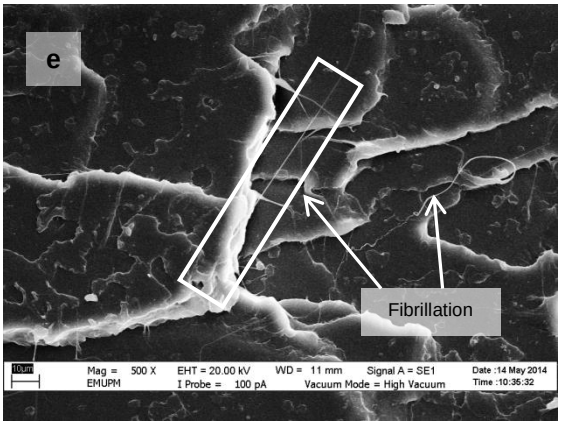
e
Fibrillation

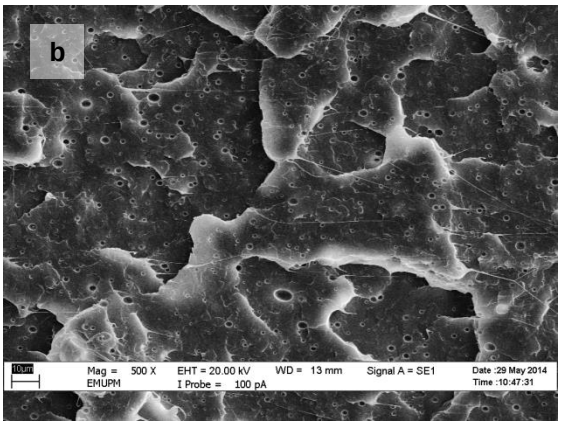
b

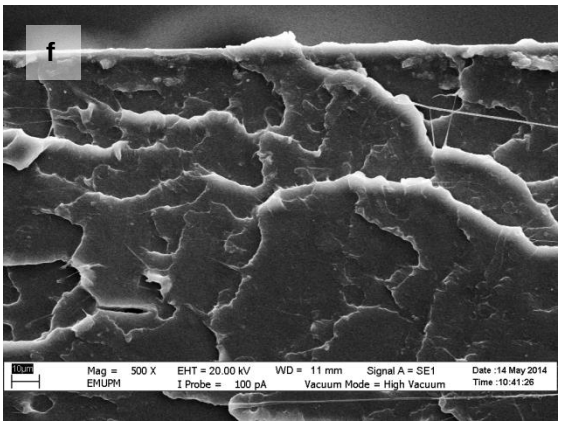
f

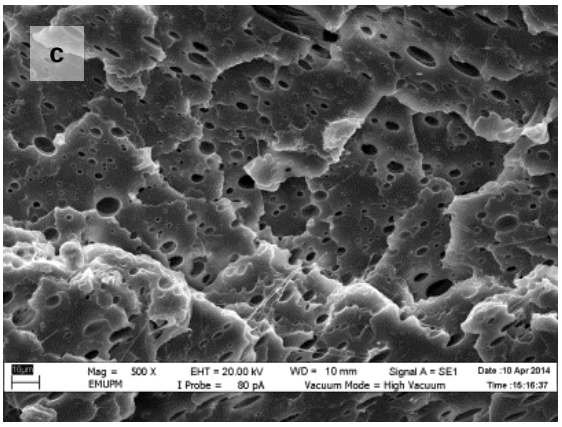
c

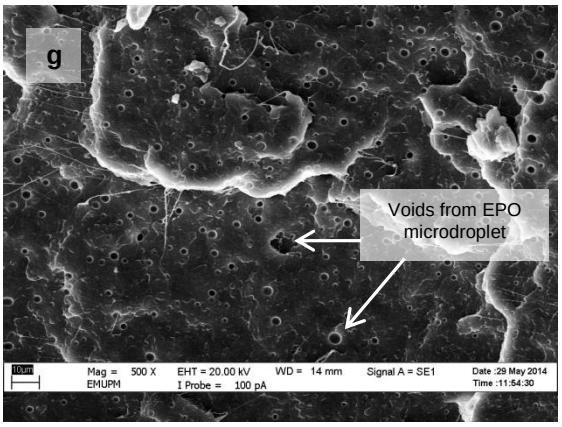
g
Voids from EPO microdroplet

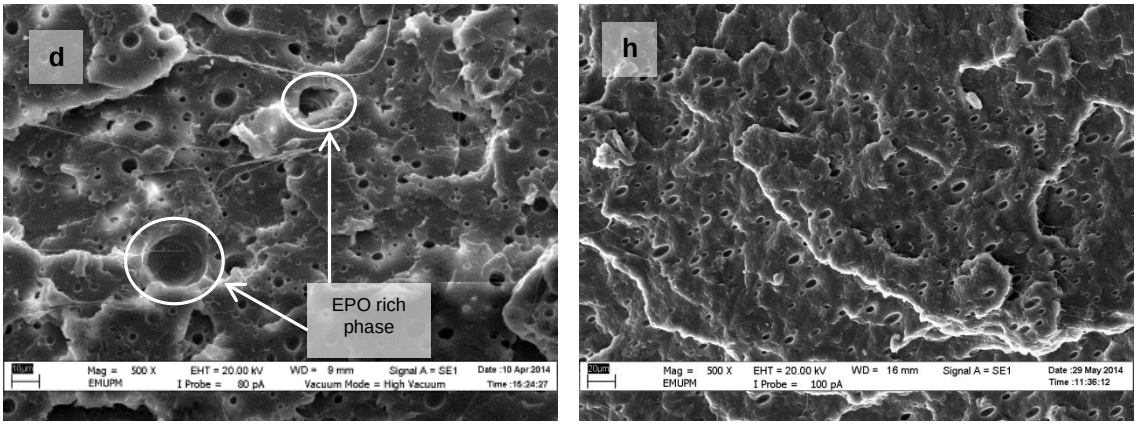

Fig. 15. VPSEM micrographs at 500x magnification of tensile fracture surface of (a) PLA/EPO3; (b) PLA/EPO5; (c) PLA/EPO10; (d) PLA/EPO15; (e) PLA/ESO3; (f) PLA/ESO5; (g) PLA/ESO10; and (h) PLA/ESO15

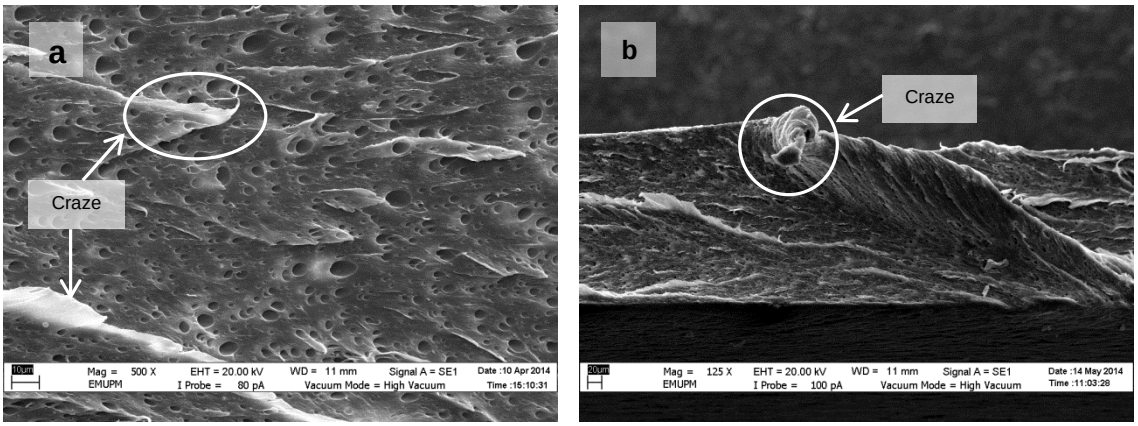

Fig. 16. VPSEM micrographs at 500x magnification of tensile fracture surface of (a) PLA/ESO15; and 250x magnification of tensile fracture surface of (b) PLA/EPO5

Conversely, no micro-droplets of ESO were observed in PLA/ESO blends within 5 wt.% of ESO addition. ESO was homogenously blended with the PLA matrix, which signified better miscibility as compared to EPO. As ESO content was increased to 10 wt.%, it formed separate phases, resulting in the formation of microvoids evenly scattered within the matrix. Further increase of ESO up to 15 wt.% caused the formation of largely deviated microvoids with more notable ESO rich phases. Yet at high loadings (10 and 15 wt.%), the accumulated microvoids from ESO was noticeably smaller than that of EPO.

The present morphology trend of PLA/ESO blends could be similar to the trend reported by Yang *et al.* (2009), where microvoids occurred when excess plasticizer was added. Yang and co-workers (2009) added dioctyl phthalate (DOP) plasticizer into cross-linked PLA. With DOP loading less than 12.5 wt.%, homogeneous blends with reduced separated aggregations of the non-cross-linked PLA and cross-linked PLA were seen. At 15 wt.%, DOP was in excess and accumulated into microvoids within the matrix. As observed in the present work, while ESO is partially miscible with PLA, inhomogeneous blend occurred at 10 wt.% of ESO.

As for PLA/EPO blend, Silverajah and co-workers (2012) also reported phase separation within the range of EPO added in PLA up to 5 wt.%. Nevertheless, Silverajah

et al. (2012) have witnessed homogenous blend with no phase separation when 1 wt.% of EPO was added into PLA. In addition, improvement in elongation at break, impact strength, and flexural strength were also reported which justified EPO's presence. From the present experimental results and other published works as mentioned above, EPO may have weaker miscibility with PLA as compared to ESO, albeit both were partially miscible.

CONCLUSIONS

1. Commercially available ESO and relatively new EPO were compared as plasticizers for PLA at various loadings. While being partially miscible to PLA, their inclusion, which significantly reinforced the ductility of PLA, facilitated the formation of more thermally stable α-form crystals than δ-form crystals without affecting PLA's melting points, and varied PLA's (oxygen and water vapour) barrier shall widen PLA's range in food packaging applications.
2. From all tests, PLA/EPO blends were notably more effective in reinforcement of properties as compared to equivalent loading of PLA/ESO blends.
3. The particularly high oxygen barrier of PLA/EPO blends may be prospective in packaging oxygen sensitive foods.
4. Overall, there is the potential of introducing EPO as polymer plasticizer in addition to the established ESO.

ACKNOWLEDGMENTS

The authors are thankful for the supply of epoxidized soybean oil (Vikoflex® 7170) from Arkema Inc., USA and epoxidized palm oil from the Advanced Oleochemical Technology Division (AOTD), Malaysian Palm Oil Board (MPOB), Malaysia. The authors also acknowledge the Universiti Putra Malaysia (Malaysia) for providing financial support under grant No. 9199816.

REFERENCES CITED

Abdellatief, A., and Welt, B. A. (2012). "Comparison of new dynamic accumulation method for measuring oxygen transmission rate of packaging against the steady-state method described by ASTM D3985," *Packag. Technol. Sci.* 26(5), 281-288. DOI: 10.1002/pts.1974

Ali, F., Chang, Y. W., Kang, S. C., and Yoon, J. Y. (2009). "Thermal, mechanical and rheological properties of poly (lactic acid)/epoxidized soybean oil blends," *Polym. Bull.* 62(1), 91-98. DOI: 10.1007/s00289-008-1012-9

Al-Mulla, E. A. J., Ibrahim, N. A. B., Shameli, K., Ahmad, M. B., and Yunus, W. M. Z. W. (2014). "Effect of epoxidized palm oil on the mechanical and morphological properties of a PLA–PCL blend," *Res. Chem. Intermed.* 40(2), 689-698. DOI: 10.1007/s11164-012-0994-y

Al-Mulla, E. A. J., Yunus, W. M. Z. W., Ibrahim, N. A. B., and Rahman, M. Z. A. (2010). "Properties of epoxidized palm oil plasticized polytlactic acid," *J. Mater. Sci*. 45(7), 1942-1946. DOI: 10.1007/s10853-009-4185-1

Arrieta, M. P., López, J., Ferrándiz, S., and Peltzer, M. A. (2013). "Characterization of PLA-limonene blends for food packaging applications," *Polym. Test*. 32(4), 760-768. DOI: 10.1016/j.polymertesting.2013.03.016

Arrieta, M. P., Samper, M. D., López, J., and Jiménez, A. (2014). "Combined effect of poly (hydroxybutyrate) and plasticizers on polylactic acid properties for film intended for food packaging," *J. Polym. Environ*. 22(4), 460-470. DOI: 10.1007/s10924-014-0654-y

Ayranci, E., and Tunc, S. (2003). "A method for the measurement of the oxygen permeability and the development of edible films to reduce the rate of oxidative reactions in fresh foods," *Food Chem.* 80(3), 423-431. DOI:10.1016/S0308-8146(02)00485-5

Bourtoom, T. (2008). "Plasticizer effect on the properties of biodegradable blend from rice starch-chitosan," *Songklanakarin J. Sci. Technol.* 30(1), 149-155.

Burgos, N., Martino, V. P., and Jiménez, A. (2013). "Characterization and ageing study of poly(lactic acid) films plasticized with oligomeric lactic acid," *Polym. Degrad. Stab.* 98(2), 651-658. DOI: 10.1016/j.polymdegradstab.2012.11.009

Butler, T., and Morris, B. A. (2013). "PE based multilayer film structures," in: *Plastic Films in Food Packaging: Materials, Technology and Applications,* S. Ebnesajjad (ed.), William Andrew Publishing, Oxford. DOI: 10.1016/b978-1-4557-3112-1.00003-x

Cao, X., Mohamed, A., Gordon, S. H., Willett, J. L., and Sessa, D. J. (2003). "DSC study of biodegradable poly (lactic acid) and poly (hydroxy ester ether) blends," *Thermochim. Acta* 406(1), 115-127. DOI: 10.1016/S0040-6031(03)00252-1

Cao, N., Yang, X., and Fu, Y. (2009). "Effects of various plasticizers on mechanical and water vapor barrier properties of gelatin films," *Food Hydrocolloids* 23(3), 729-735. DOI: 10.1016/j.foodhyd.2008.07.017

Carvalho, R. A., and Grosso, C. R. F. (2004). "Characterization of gelatin based films modified with transglutaminase, glyoxal and formaldehyde," *Food Hydrocolloids*. 18(5), 717–726. DOI: 10.1016/j.foodhyd.2003.10.005

Chieng, B. W., Ibrahim, N. A., Wan Yunus, W. M. Z., Hussein, M. Z., and Silverajah, V. S. (2012). "Graphene nanoplatelets as novel reinforcement filler in poly (lactic acid)/epoxidized palm oil green nanocomposites: Mechanical properties," *Int. J. Mol. Sci.* 13(9), 10920-10934. DOI: 10.3390/ijms130910920

Chua, S. C., Xu, X., and Guo, Z. (2012). "Emerging sustainable technology for epoxidation directed toward plant oil-based plasticizers," *Process Biochem.* 47(10), 1439-1451. DOI: 10.1016/j.procbio.2012.05.025

Courgneau, C., Domenek, S., Guinault, A., Avérous, L., and Ducruet, V. (2011). "Analysis of the structure-properties relationships of different multiphase systems based on plasticized poly (lactic acid)," *J. Polym. Environ.* 19(2), 362-371. DOI: 10.1007/s10924-011-0285-5

Dai, X., Xiong, Z., Na, H., and Zhu, J. (2014). "How does epoxidized soybean oil improve the toughness of microcrystalline cellulose filled polylactide acid composites?" *Compos. Sci. Technol.* 90, 9-15. DOI: 10.1016/j.compscitech.2013.10.009

Fenollar, O., García, D., Sánchez, L., López, J., and Balart, R. (2009). "Optimization of the curing conditions of PVC plastisols based on the use of an epoxidized fatty acid ester plasticizer," *Eur. Polym. J.* 45(9), 2674-2684. DOI: 10.1016/j.eurpolymj.2009.05.029

Fischer, E. W., Sterzel, H. J., and Wegner, G. K. Z. Z. (1973). "Investigation of the structure of solution grown crystals of lactide copolymers by means of chemical reactions," *Kolloid Z. Z. Polym.* 251(11), 980-990. DOI: 10.1007/BF01498927

Figura, L. O., and Teixeira, A. A. (2007). "Permeability," in: *Food Physics (Physical Properties - Measurement and Applications)*, Springer-Verlag Berlin Heidelberg, Berlin.

Gamage, P. K., O'Brien, M., and Karunanayake, L. (2009). "Epoxidation of some vegetable oils and their hydrolysed products with peroxyformic acid-optimised to industrial scale," *J. Natl. Sci. Found. Sri Lanka* 37, 229-240.

García, M. A., Martino, M. N., and Zaritzky, N. E. (2000). "Lipid addition to improve barrier properties of edible starch-based films and coatings," *J. Food Sci.* 65(4), 941-944. DOI: 10.1111/j.1365-2621.2000.tb09397.x

Ghosh, S. B., Bandyopadhyay-Ghosh, S., and Sai, M. (2010). "Composites," in: *Poly(lactic acid): Synthesis, Structures, Properties, Processing, and Applications*, 2nd Ed., Auras, R., Lim, L. T., Selke, S. E .M., and Tsuji, H. (eds.), John Wiley & Sons, Hoboken, New Jersey. DOI: 10.1002/9780470649848.ch18

Groshart, C., and Okkerman, P. C. (2000). "Towards the establishment of a priority list of substances for further evaluation of their role in endocrine disruption," European Commission Dg Env. DOI:M0355008/1786Q/10/11/00

HallStar (2007). *PLASTHALL® P-550 Plasticizer for Refrigerator Gaskets*, HallStar, (http://www.hallstar.com/techdocs/plasthall_p550_for_refrigerator_gaskets.pdf).

Jia, P.-Y., Bo, C.-Y., Hu, L-.H., and Zhou, Y.-H. (2014). "Properties of poly(vinyl alcohol) plasticized by glycerin," *J. For. Prod. Ind.* 3(3), 151-153.

Kulinski, Z., and Piorkowska, E. (2005). "Crystallization, structure and properties of plasticized poly (L-lactide)," *Polymer* 46(23),10290-10300. DOI: 10.1016/j.polymer.2005.07.101

Kulinski, Z., Piorkowska, E., Gadzinowska, K., and Stasiak, M. (2006). "Plasticization of poly (L-lactide) with poly (propylene glycol)," *Biomacromolecules* 7(7), 2128-2135. DOI: 10.1021/bm060089m

Laboulfie, F., Hemati, M., Lamure, A., and Diguet, S. (2013). "Effect of the plasticizer on permeability, mechanical resistance and thermal behaviour of composite coating films," *Powder Technol*. 238, 14-19. DOI: 10.1016/j.powtec.2012.07.035

Lathi, P. S., and Mattiasson, B. (2007). "Green approach for the preparation of biodegradable lubricant base stock from epoxidized vegetable oil," *Appl. Catal. B* 69(3), 207-212. DOI: 10.1016/j.apcatb.2006.06.016

Liu, L., Kerry, J. F., and Kerry, J. P. (2006). "Effect of food ingredients and selected lipids on the physical properties of extruded edible films/casings," *Int. J. Food Sci. Tech.* 41(3), 295-302. DOI: 10.1111/j.1365-2621.2005.01063.x

Maizatul, N., Norazowa, I., Yunus, W. M. Z. W., Khalina, A., and Khalisanni, K. (2013). "FTIR and TGA analysis of biodegradable poly (lactic acid)/treated kenaf bast fibre: Effect of plasticizers," *Pertanika J. Sci. Technol.* 21(1), 151-160.

Markarian, J. (2007). "PVC additives- What lies ahead?" *Plast. Addit. Compd.* 9(6), 22-25. DOI: 10.1016/S1464-391X(07)70153-8

Martin, O., and Averous, L. (2001). "Poly(lactic acid): Plasticization and properties of biodegradable multiphase systems," *Polymer* 42(14), 6209-6219. DOI: 10.1016/S0032-3861(01)00086-6

Masirek, R., Kulinski, Z., Chionna, D., Piorkowska, E., and Pracella, M. (2007). "Composites of poly(L-lactide) with hemp fibers: Morphology and thermal and mechanical properties," *J. Appl. Polym. Sci.* 105(1), 255-268. DOI: 10.1002/app.26090

Mekonnen, T., Mussone, P., Khalil, H., and Bressler, D. (2013). "Progress in bio-based plastics and plasticizing modifications," *J. Mater. Chem. A* 1(43), 13379-13398. DOI: 10.1039/c3ta12555f

Mohan (2011a). *Danone First to Switch to PLA for Yogurt Cup in Germany*, GreenerPackage.com (http://www.greenerpackage.com/bioplastics/danone_first_switch_pla_yogurt_cup_germany)

Mohan 2011b). *PLA Yogurt Cup Project Scrutinized from All Angles*, GreenerPackage.com (http://www.greenerpackage.com/bioplastics/pla_yogurt_cup_project_scrutinized_all_angles)

Murariu, M., Ferreira, A. D. S., Alexandre, M., and Dubois, P. (2008). "Polylactide (PLA) designed with desired end-use properties: 1. PLA compositions with low molecular weight ester-like plasticizers and related performances," *Polym. Adv. Technol*. 19(6), 636-646. DOI: 10.1002/pat.1131

Pillin, I., Montrelay, N., and Grohens, Y. (2006). "Thermo-mechanical characterization of plasticized PLA: Is the miscibility the only significant factor?," *Polymer* 47(13), 4676-4682. DOI: 10.1016/j.polymer.2006.04.013

Piorkowska, E., Kulinski, Z., Galeski, A., and Masirek, R. (2006). "Plasticization of semicrystalline poly (L-lactide) with poly (propylene glycol)," *Polymer* 47(20), 7178-7188. DOI: 10.1016/j.polymer.2006.03.115

Silverajah, V. S., Ibrahim, N. A., Zainuddin, N., Yunus, W. M. Z. W., and Hassan, H. A. (2012). "Mechanical, thermal and morphological properties of poly (lactic acid)/epoxidized palm olein blend," *Molecules* 17(10), 11729-11747. DOI: 10.3390/molecules171011729

Srinivasa, P. C., Ramesh, M. N., and Tharanathan, R. N. (2007). "Effect of plasticizers and fatty acids on mechanical and permeability characteristics of chitosan films," *Food Hydrocolloids* 21(7), 1113-1122. DOI: 10.1016/j.foodhyd.2006.08.005

Tee, Y. B., Talib, R. A., Abdan, K., Chin, N. L., Basha, R. K., and Yunos, K. F. M. (2014). "Toughening poly(lactic acid) and aiding the melt-compounding with bio-sourced plasticizers," *Agric. Agric. Sci. Procedia* 2, 289-295. DOI: 10.1016/j.aaspro.2014.11.041

Téllez, G. L., Vigueras-Santiago, E., and Hernández-López, S. (2009). "Characterization of linseed oil epoxidized at different percentages," *Superficies Y Vacío* 22(1), 5-10.

Wang, Q., Chen, Y., Tang, J., and Zhang, Z. (2013). "Determination of the solubility parameter of epoxidized soybean oil by inverse gas chromatography," *J. Macromol. Sci. Part B* 52(10), 1405-1413. DOI: 10.1080/00222348.2013.768870

Wang, Z., Hou, X., Mao, Z., Ye, R., Mo, Y., and Finlow, D. E. (2008). "Synthesis and characterization of biodegradable poly (lactic acid-co-glycine) via direct melt copolymerization," *Iran. Polym. J.* 17(10), 791-798.

Wasanasuk, K., and Tashiro, K. (2011). "Crystal structure and disorder in Poly (l-lactic acid) δ form (α′ form) and the phase transition mechanism to the ordered α form," *Polymer* 52(26), 6097-6109. DOI: 10.1016/j.polymer.2011.10.046

Xiong, Z., Yang, Y., Feng, J., Zhang, X., Zhang, C., Tang, Z., and Zhu, J. (2013). "Preparation and characterization of poly (lactic acid)/starch composites toughened with epoxidized soybean oil," *Carbohydr. Polym.* 92(1), 810-816. DOI: 10.1016/j.carbpol.2012.09.007

Xu, Y. Q., and Qu, J. P. (2009). "Mechanical and rheological properties of epoxidized soybean oil plasticized poly (lactic acid)," *J. Appl. Polym. Sci*. 112(6), 3185-3191. DOI: 10.1002/app.29797

Yang, S. L., Wu, Z. H., Meng, B., and Yang, W. (2009). "The effects of dioctyl phthalate plasticization on the morphology and thermal, mechanical, and rheological properties of chemical crosslinked polylactide," *J. Polym. Sci., Part B: Polym. Phys*. 47(12), 1136-1145. DOI: 10.1002/polb.21716

Zakaria, Z., Islam, M. S., Hassan, A., Mohamad Haafiz, M. K., Arjmandi, R., Inuwa, I. M., and Hasan, M. (2013). "Mechanical properties and morphological characterization of PLA/chitosan/epoxidized natural rubber composites," *Adv. Mater. Sci. Eng.* 2013, 1-7. DOI: 10.1155/2013/629092

Article submitted: September 4, 2015; Peer review completed: November 8, 2015; Revised version received and accepted: December 10, 2015; Published: December 17, 2015.
DOI: 10.15376/biores.11.1.1518-1540